
Inverse Renormalization Group Transformation in Bayesian Image Segmentations

Kazuyuki Tanaka ^{*1}, Shun Kataoka¹, Muneki Yasuda², Masayuki Ohzeki³

¹*Graduate School of Information Sciences, Tohoku University, 6-3-09*

Aramaki-aza-aoba, Aoba-ku, Sendai 980-8579, Japan

²*Graduate School of Science and Engineering, Yamagata University, 4-3-16 Jyounan,
Yonezawa 992-8510, Japan*

³*Graduate School of Informatics, Kyoto University, 36-1 Yoshida-Honmachi,
Sakyo-ku, Kyoto 606-8501 Japan*

A new Bayesian image segmentation algorithm is proposed by combining a loopy belief propagation with an inverse real space renormalization group transformation to reduce the computational time. In results of our experiment, we observe that the proposed method can reduce the computational time to less than one-tenth of that taken by conventional Bayesian approaches.

KEYWORDS: statistical-mechanical informatics, Markov random fields, renormalization group

Bayesian segmentation modeling based on Markov random fields (MRF's) is one of the interesting research topics¹⁾. Image segmentations are required to classify pixels in an observed image into several regions, and such segmentations are regarded as a kind of clustering of pixels. Markov random fields are regarded as classical spin systems in statistical mechanics²⁾. Loopy belief propagations (LBP's) have been applied to construct certain practical algorithms for application in Bayesian image segmentations^{3,4)}. In the present short note, we propose a new Bayesian image segmentation algorithm based on a RSRG transformation to reduce the computational time.

We consider an image as defined on a set of pixels arranged on a square grid graph $(\mathcal{V}, \mathcal{E})$. Here $\mathcal{V} \equiv \{i | i = 1, 2, \dots, |\mathcal{V}|\}$ denotes the set of all the pixels and \mathcal{E} is the set of all the nearest-neighbour pairs of pixels $\{i, j\}$. The total numbers of elements in the sets \mathcal{V} and \mathcal{E} are denoted by $|\mathcal{V}|$ and $|\mathcal{E}|$, respectively. The square grid graph has the periodic boundary conditions along the x - and y -directions. The label at each pixel i is regarded

^{*}E-mail: kazu@smapi.is.tohoku.ac.jp

as a state variable, and it is denoted by a_i . Each pixel i takes on the values of all the possible integers in the set $\mathcal{Q} \equiv \{0, 1, 2, \dots, q-1\}$ as its region label. The state vector of labels is represented by $\mathbf{a} = (a_i | i \in \mathcal{V}) = (a_1, a_2, \dots, a_{|\mathcal{V}|})^T$. The prior probability of a labeling configuration \mathbf{a} is assumed to be specified by a constant u as

$$P(\mathbf{a}) \propto \prod_{\{i,j\} \in \mathcal{E}} \exp\left(\frac{1}{2}\alpha\delta_{a_i,a_j}\right), \quad (1)$$

up to the normalization constant.

For the prior probability distribution $P(\mathbf{a}|u)$, we introduce the following RSRG transformation:

$$\exp\left(\frac{1}{2}\alpha^{(r)}\delta_{a_1,a_3}\right) \propto \sum_{a_2 \in \mathcal{Q}} \sum_{a_4 \in \mathcal{Q}} \exp\left(\frac{1}{2}\alpha^{(r-1)}(\delta_{a_1,a_2} + \delta_{a_2,a_3} + \delta_{a_1,a_4} + \delta_{a_4,a_3})\right) \quad (r = 1, 2, \dots, R), \quad (2)$$

where $\alpha^{(0)} \equiv \alpha$. The square grid graph $\mathcal{G}^{(r)} = (\mathcal{V}^{(r)}, \mathcal{E}^{(r)})$ is defined as shown in Fig.1(b). Here $\mathcal{V}^{(r)}$ is the set of all the pixels and $\mathcal{E}^{(r)}$ represents the set of all the nearest-neighbour pairs of pixels $\{i, j\}$ in the graph $\mathcal{G}^{(r)}$. Here, we remark that $\mathcal{V}^{(r)}$ is the subset of \mathcal{V} . The prior probability distribution $P^{(r)}(\mathbf{a}^{(r)})$ for $\mathbf{a}^{(r)} \equiv (a_i | i \in \mathcal{V}^{(r)})$ on $\mathcal{G}^{(r)} = (\mathcal{V}^{(r)}, \mathcal{E}^{(r)})$ after the r -iteration of the RSRG transformation is expressed as

$$P^{(r)}(\mathbf{a}^{(r)}) \propto \prod_{\{i,j\} \in \mathcal{E}^{(r)}} \exp\left(\frac{1}{2}\alpha^{(r)}\delta_{a_i,a_j}\right), \quad (3)$$

up to the normalization constant. The transformation in Eq.(2) can be reduced to

$$\alpha^{(r)} = 4 \ln\left(\frac{q-1 + e^{\alpha^{(r-1)}}}{q-2 + 2e^{\frac{1}{2}\alpha^{(r-1)}}}\right). \quad (4)$$

The intensities of the red, green, and blue channels at pixel i in the observed image are regarded as state variables denoted by d_i^{Red} , d_i^{Green} and d_i^{Blue} , respectively. The random fields of red, green and blue intensities in the observed color image are then represented by the $3|\mathcal{V}|$ -dimensional vector $\mathbf{d} \equiv (\mathbf{d}_1, \mathbf{d}_2, \dots, \mathbf{d}_{|\mathcal{V}|})^T$, where $\mathbf{d}_i \equiv (d_i^{\text{Red}}, d_i^{\text{Green}}, d_i^{\text{Blue}})^T$. The state variables d_i^{Red} , d_i^{Green} and d_i^{Blue} at each pixel i can take any real numbers in the interval $(-\infty, +\infty)$. It is to be noted that, in the above generative process of natural color images, we assign each pixel i to a labeling state a_i . For example, if the pixel i is in the labeling state $a_i = \xi$ ($\xi \in \mathcal{Q}$), then its color intensity

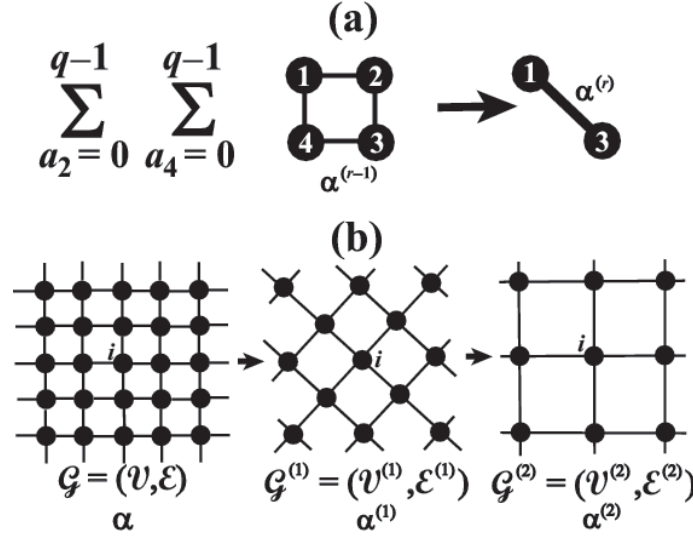


Fig. 1. Block spin transformation. (a) Graphical representation of Eq.(2). (b) $\mathcal{G}^{(r)} = (\mathcal{V}^{(r)}, \mathcal{E}^{(r)})$ ($r = 1, 2, \dots$) in the coarse-graining process.

vector \mathbf{d}_i is assumed to be generated from the following Gaussian distribution:

$$g(\mathbf{d}_i|\xi) \equiv \sqrt{\frac{1}{\det(2\pi\mathbf{C}(\xi))}} \exp\left(-\frac{1}{2}(\mathbf{d}_i - \mathbf{m}(\xi))^T \mathbf{C}^{-1}(\xi)(\mathbf{d}_i - \mathbf{m}(\xi))\right). \quad (5)$$

In other words, the labeling state a_i specifies the distribution within the set $\{g(\mathbf{d}_i|\xi)|\xi \in \mathcal{Q}\}$ that generates a color intensity vector \mathbf{d}_i . As mentioned in the previous section, we introduce the labeling state variable a_i at each pixel i as a Potts spin variable in statistical mechanics.

After setting R as a positive integer, we construct a $3|\mathcal{V}^{(R)}|$ -dimensional vector $\mathbf{d}^{(R)} = (\mathbf{d}_i | i \in \mathcal{V}^{(R)})$ from our observed color image \mathbf{d} . We remark that d_i in the coarse-grained image $\mathbf{d}^{(R)}$ is always the same as d_i in the observed color image \mathbf{d} in our scheme. By using the Bayes formula, we introduce the posterior probability distribution $P(\mathbf{a}^{(R)}|\mathbf{d}^{(R)})$ for $\mathbf{a}^{(R)} = (a_i | i \in \mathcal{V}^{(R)})$ as follows:

$$P^{(R)}(\mathbf{a}^{(R)}|\mathbf{d}^{(R)}) \propto \left(\prod_{i \in \mathcal{V}^{(R)}} g(\mathbf{d}_i|a_i)\right) \left(\prod_{\{i,j\} \in \mathcal{E}^{(R)}} \exp\left(\frac{1}{2}\alpha^{(R)}\delta_{a_i,a_j}\right)\right), \quad (6)$$

up to the normalization constant. The estimates $\hat{\alpha}^{(R)}$ and $\{\widehat{\mathbf{m}}(\xi), \widehat{\mathbf{C}}(\xi)|\xi \in \mathcal{Q}\}$ of $\alpha^{(R)}$ and $\{\mathbf{m}(\xi), \mathbf{C}(\xi)|\xi \in \mathcal{Q}\}$ are approximately computed by means of the LBP algorithm for the conditional maximum entropy framework⁴. After obtaining these estimates, we calculate $\hat{\alpha}^{(0)}$ from $\hat{\alpha}^{(R)}$ by using the following inverse RSRG transformations of Eq.(4):

$$\hat{\alpha}^{(r-1)} = 2\ln\left(e^{\frac{1}{4}\hat{\alpha}^{(r)}} + \sqrt{(e^{\frac{1}{4}\hat{\alpha}^{(r)}} + Q - 1)(e^{\frac{1}{4}\hat{\alpha}^{(r)}} - 1)}\right) \quad (r = R, \dots, 2, 1), \quad (7)$$

where $\hat{\alpha} = \hat{\alpha}^{(0)}$.

Given the estimates $\hat{\alpha}$ and $\{\widehat{\mathbf{m}}(\xi), \widehat{\mathbf{C}}(\xi) | \xi \in \mathcal{Q}\}$, the estimate of labeling $\hat{\mathbf{a}}(\mathbf{d}) = (\hat{a}_1(\mathbf{d}), \hat{a}_2(\mathbf{d}), \dots, \hat{a}_{|\mathcal{V}|}(\mathbf{d}))^T$ is determined by

$$\hat{a}_i(\mathbf{d}) \equiv \operatorname{argmax}_{\zeta \in \mathcal{Q}} \sum_{\mathbf{a}} \delta_{a_i, \zeta} P^{(0)}(\mathbf{a} | \mathbf{d}) \quad (i \in \mathcal{V}). \quad (8)$$

This procedure to determine the estimate $\hat{\mathbf{a}}(\mathbf{d})$ is approximately computed by using the LBP algorithm to $P^{(0)}(\mathbf{a} | \mathbf{d})$.

We show numerical experiments by our proposed approach in Fig.2. In our numerical experiments, the test image \mathbf{d} in Fig.2(a) is acquired from the Berkeley Segmentation Data Set 500 (BSDS500)⁵. The size of the test image \mathbf{d} is 321×481 and the sizes of $\mathbf{d}^{(R)}$ are reduced to 20×30 for $R = 8$ and 10×20 for $R = 10$. The labeling configurations $\hat{\mathbf{a}}$ obtained by means of our proposed algorithm based on our inverse RSRG transformation for $R = 8$ and $R = 10$ are shown in Figs.2(b) and (c), respectively. In our proposed algorithm, $\hat{\mathbf{a}}^{(R)}$ and $\{\widehat{\mathbf{m}}(\xi), \widehat{\mathbf{C}}(\xi) | \xi \in \mathcal{Q}\}$ for $\mathbf{d}^{(R)}$ are estimated by using the conditional maximum entropy framework with the LBP such that they are obtained by subjecting $\mathbf{d}^{(R)}$ to the algorithm presented in §3 of Ref.⁴. The estimates $\hat{\alpha}^{(R)}$ for $R = 8$ and $R = 10$ are 2.5288 and 2.5039, respectively. The estimates $\hat{\alpha} = \hat{\alpha}^{(0)}$ obtained by means of the inverse RSRG group transformations given by Eq.(7) for $R = 8$ and $R = 10$ are 3.6765 and 3.6797, respectively. The labeling configuration in Fig.2(d) is computed directly by applying \mathbf{d} to the algorithm in §3 of Ref.⁴. The estimate $\hat{\alpha}$ of α in Fig.2(d) is 3.0301. The computational times corresponding to Figs.2(b)-(d) are 128(Sec), 78(Sec) and 1331(Sec), respectively. Our numerical experiments were performed by using a personal computer with an Intel(R) Core(TM) i7-4600U CPU with a memory of 8GB. From the results of our experiment, we observe that the computational time can be reduced to less than one-tenth of that taken by conventional methods by application of our proposed algorithm based on the inverse RSRG transformation. We obtained results similar to the above mentioned case for other test images in the database set of BSDS500.

In the present short note, we have presented a novel algorithm that involve the combination of the inverse RSRG transformation with the Bayesian image segmentation method proposed in Ref.⁴. Our proposed method can reduce the computational time of the hyperparameter estimations significantly. We expect that our approach can also be applied to Bayesian image segmentations for three-dimensional computer vision, which remains one of significant problems.

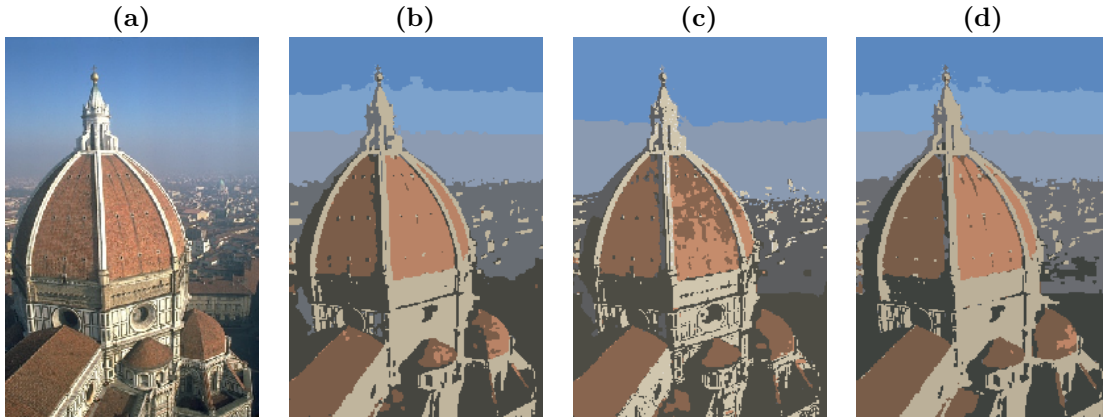


Fig. 2. Image segmentations in the case of $q = 8$. (a) Test image \mathbf{d} from the database of Ref.⁵. (b)-(c) Labeling configurations by our proposed algorithm based on our inverse RSRG transformation for (b) $R = 8$ and (c) $R = 10$. (c) Labeling configuration by Ref.⁴ without using the inverse RSRG transformation. The results in (b)-(d) are shown with the color $\widehat{\mathbf{m}}(\widehat{a}_i(\mathbf{d}), \mathbf{d})$ at each pixel i for the test image \mathbf{d} .

Acknowledgements

The authors are grateful to Prof. Federico Ricci-Tersenghi of the Department of Physics, University of Roma La Sapienza for valuable comments. This work was partly supported by the JST-CREST and the Grants-In-Aid (No.25280089) for Scientific Research from the Ministry of Education, Culture, Sports, Science and Technology of Japan.

References

- 1) Z. Kato and J. Zerubia: Foundations and Trends in Signal Processing, **5** (2012) 1.
- 2) K. Tanaka: J. Phys. A **35** (2002) R81.
- 3) R. Hasegawa, M. Okada and S. Miyoshi: J. Phys. Soc. Jpn **80** (2011) 093802.
- 4) K. Tanaka, S. Kataoka, M. Yasuda, Y. Waizumi and C.-T. Hsu: J. Phys. Soc. Jpn **83** (2014) 124002.
- 5) P. Arbelaez, M. Maire, C. Fowlkes and J. Malik: IEEE Trans. Pattern Anal. Mach. Intell. **33** (2011) 898.